Pressure drop in a prototypical 3D magnetohydrodynamic flow across contraction of a fusion blanket manifold

T. Rhodes, S. Smolentsev*

University of California - Los Angeles, USA

Abstract. Quantifying and predicting 3D magnetohydrodynamic (MHD) pressure losses associated with liquid metal flows in complex geometry ducts is required to effectively design breeding blankets for fusion reactors. Of such complex geometry components, manifolds exhibit major pressure losses in the blanket due to sudden changes in the flow geometry and associated 3D induced electric currents. Recent correlations [T. Rhodes *et al*., Magnetohydrodynamic pressure drop and flow balancing of liquid metal flow in a prototypic fusion blanket manifold, Physics of Fluids, 30 (2018) 057101.] demonstrate promise for predicting pressure drops in electrically insulated inlet manifolds, which feature sudden expansions of the duct geometry along the magnetic field direction. In the present work, the extent to which these correlations can be applied to electrically insulated outlet manifolds, which feature sudden contractions, is investigated in both viscous-electromagnetic (VE) and inertial-electromagnetic (IE) regimes for Reynolds numbers $50 < Re < 1500$, Hartmann numbers $2500 < Ha < 5475$, and expansion/contraction ratio 10. Using the MHD solver HIMAG to numerically simulate eutectic lead-lithium (PbLi) flows in ducts with expansions and contractions under strong magnetic fields, the pressure losses are shown to be nearly identical with slightly higher magnitudes in the contraction cases. The small discrepancy in the MHD pressure drop between contractions and expansions (<8%) suggests that the earlier obtained correlations for the 3D MHD pressure drop in a duct flow with a sudden expansion are also applicable to the duct flows with a sudden contraction.

Keywords: Liquid Metal Magnetohydrodynamics, Manifold, Sudden Contraction, Pressure Drop, Blanket

1. Introduction

Liquid metal (LM) breeding blankets of fusion power reactors circulate pure lithium (Li) or Li-containing LMs such as eutectic lead-lithium (PbLi) alloy to breed tritium and harness heat energy. The LM is both fed to and collected from multiple parallel channels inside the blankets via manifolds where, due to the reactor's strong plasma-confining magnetic field, significant 3D magnetohydrodynamic (MHD) interactions between the flowing LM and the magnetic field are known to cause high MHD pressure drops [1]. Several designs of inlet and outlet manifolds have been proposed in engineering blanket studies, in particular for Dual Coolant Lead Lithium (DCLL) blankets, where PbLi alloy circulates through long poloidal ducts at moderate velocities of ~ 10 cm/s for tritium breeding and power conversion [2]. Of the proposed manifold designs, the most attractive one uses a co-axial pipe for supplying "cold" breeder to the blanket entrance through the annulus of the co-axial pipe and taking out "hot" PbLi from the blanket exit towards the ancillary equipment through the inner pipe [3]. Such a design has several potential advantages over other designs, including reduced size, lower inner steel wall temperature, and lower tritium loss from the PbLi breeder. However, this design has potential issues associated with possibly high MHD pressure drop due to electromagnetic coupling between the LM flow inside the annulus and that in the inner pipe which have not been fully resolved yet [4]. A conservative manifold design [5] relies on two separate manifolds at the blanket inlet and outlet, and correspondingly, one inlet and one outlet pipe to feed

* Corresponding author: Sergey Smolentsev (*sergey@fusion.ucla.edu*)

the module and to extract PbLi from the blanket. For such a manifold solution, the MHD pressure drop is expected to be lower compared to the novel design that has a co-axial pipe supply system but the pressure drop is still expected to be high due to large 3D MHD pressure drops that occur when the LM flow undergoes expansion or contraction along the magnetic field direction and these are estimated to account for about half the entire pressure drop of the blanket [5].

There has been a decent number of computational studies [6-14] of prototypical manifold-like MHD flows that varied in flow geometry (flows with expansions or contractions, and with and without the parallel channels), wall electrical conductivity (electrically conducting versus insulating walls), magnetic field direction (geometry changes are either in the plane perpendicular or parallel to the magnetic field) and range of flow parameters (various Hartmann *Ha*, and Reynolds *Re,* numbers). Of the particular importance in these studies, was the characterization of the MHD pressure drop as it can significantly limit the LM blanket design window. In the full 3D computations, the Hartmann number was typically limited to several hundreds, rarely to a few thousands, while the Reynolds number was set at several thousands or less. These limitations in magnitudes of the flow parameters are due to various numerical issues [15] and the need for extremely high computational resources at high *Ha* and *Re* associated with the fine resolution of MHD boundary layers, such as the Hartmann layers at the duct walls perpendicular to the magnetic field and internal shear layers. Asymptotic techniques allow computations for much higher *Ha*, but their range of applicability is limited [6,7]. Almost all numerical studies have been performed for flows in ducts with expansions and, to our best knowledge, only two of them for contractions [7,13]. Typically, higher MHD pressure drops were observed for the ducts that featured sudden geometry changes in the plane parallel to the applied magnetic field compared to the perpendicular field orientation. Also, much higher MHD pressure drops occur in electrically conducting ducts compared to the ducts with insulating walls. The true blanket manifold case involves geometrical changes in the plane parallel to the applied (toroidal) magnetic field and electrically insulating walls as in the case of the DCLL blanket, where insulating flow channel inserts (FCIs) are used to electrically decouple the PbLi flow from the more conducting steel structure. This model was implemented in [14] and also in the present studies. An interesting approach to the characterization of the MHD pressure drop in the flows with contractions and expansions was utilized in the two studies by Kumamuru [12, 13], where the extended Bernoulli equation was used to analyze the magnetic field effect via the loss coefficient at maximum *Ha*=500 and maximum *Re*=5000. As shown in these studies, the loss coefficient in the contraction flows generally becomes larger than that in the case of corresponding expansions but the difference is not significant. An experimental study of MHD flows in a duct with expansion was performed in [16].

Rhodes *et al*. [14] have performed detailed computational study of the MHD pressure drop for the PbLi inlet manifold. It was concluded that almost all MHD pressure drop occurs in the expansion region of the manifold, while the MHD pressure drops associated with the flow redistribution from the expansion region into parallel poloidal ducts and that due to the radial-poloidal change in the flow direction are significantly smaller. This conclusion allowed for further reduction of the MHD pressure drop analysis to focusing on the flow in the expansion region only. As a result of many 3D computations over a range of *Ha* and *Re* numbers and expansion ratios, accurate correlations were established for estimating the 3D MHD pressure drop in electrically insulated ducts across sudden expansions of the inlet manifold. In doing so, two flow regimes (originally postulated by Hunt and Leibovich [17]) were observed: (1) an inertial-electromagnetic (IE) regime characterized by the balance of inertia and Lorentz forces inside the 3D MHD disturbance at the sudden change in duct aspect ratio, and (2) a viscous-electromagnetic (VE) regime characterized by the balance of viscous and Lorentz forces inside the 3D MHD disturbance. As determined in Ref. [14], flows with $Re/\sqrt{Ha}$ >3 are in the IE regime while those with $Re/\sqrt{Ha}$ <3 are in the VE regime. Most of the blanket flows are expected to be in the IE regime where inertial forces are especially important.

In the present work, we investigate the degree to which the 3D MHD pressure drop correlations established in Ref. [14] for the inlet manifold are applicable to sudden contractions of the electrically insulated outlet manifold which has the same geometry as the inlet manifold but with reversed flow

direction. Obtained results can be used in future designs of inlet and outlet manifolds as well as to support manifold designs that use a co-axial pipe as such designs also feature flow expansions and contractions.

2. Numerical methodology

Solutions of laminar MHD duct flows in a transverse magnetic field are obtained numerically by marching in time. The computations are continued until a steady state flow is achieved. In all computed cases, the flow reaches a steady state as the applied magnetic field is strong (high *Ha* numbers) while the flow velocities are relatively low (low *Re* numbers).

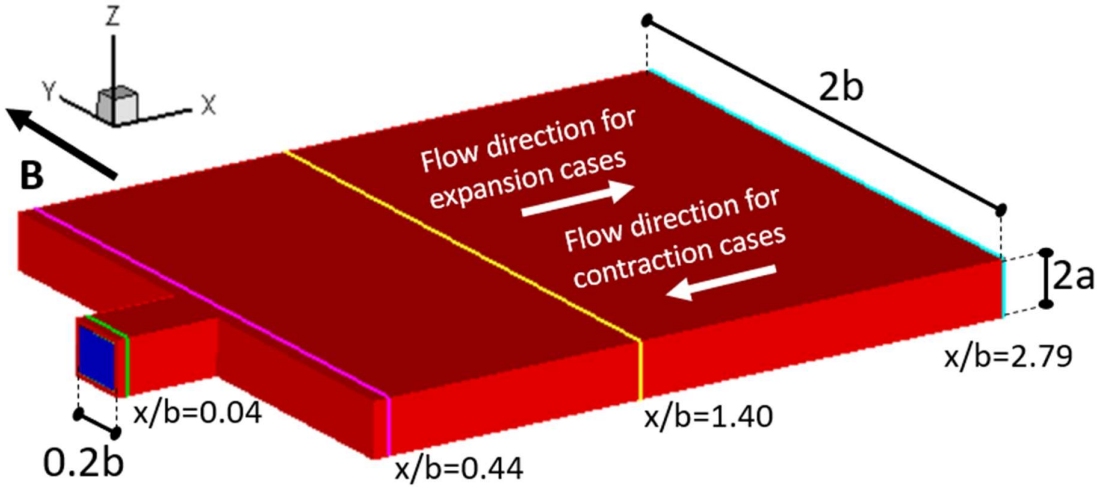

Figure 1. The simulation geometry is a duct with a sudden expansion or contraction depending on the flow direction. The flow in the inlet manifold features expansion (the flow direction is from left to right), while the flow in the outlet manifold (the flow direction is from right to left) experiences contraction.

Flows through electrically non-conducting ducts featuring a 10x sudden expansion that occurs in the direction of the applied magnetic field are considered along with those featuring the same 10x sudden contraction. The simulation geometry (Fig. 1) is the same for each scenario, the key difference being the flow direction ($U > 0$ for sudden expansions and $U < 0$ for sudden contractions).

The MHD duct flows studied here are characterized by dimensionless parameters Hartmann number *Ha*, and Reynolds number *Re*. The Hartmann number squared represents the ratio between electromagnetic and viscous forces: $Ha = bB\sqrt{\sigma/\mu}$, where b is the maximum halfwidth of the duct along the magnetic field direction, B is the applied magnetic field strength, σ is the electrical conductivity of the fluid, and μ is the dynamic viscosity. The Reynolds number represents the ratio between inertial and viscous forces: $Re = \frac{\rho bU}{\mu}$, where U is the magnitude of the mean velocity in the widest region of the duct, and ρ is the fluid density. In addition, an interaction parameter (Stuart number) can be constructed as $N=Ha^2/Re$ that represents the ratio between electromagnetic and inertia forces. Also, for all the present cases, $\frac{a}{b} = 0.08$, where a is the halfwidth of the duct perpendicular to the magnetic field and mean flow direction as shown in Fig.1. The computations were run in parallel using 1024 nodes of EDISON, a supercomputer at the National Energy Research Scientific Computing Center (NERSC). Calculations were performed with a timestep size of $\Delta t=10^{-4}$s until steady state solutions were reached as indicated by the L2 norms of the residuals reaching the order of 10^{-10}. Here, residuals are defined as the difference of flow variables at consecutive time steps. For

cases with the highest Hartmann number, Ha=5475, a timestep size of Δt=10^{-5}s was required for convergence.

2.1. *Governing equations*

Similar to the mathematical formulation in Ref. [14], the problem for the PbLi flow in the contraction region is governed by equations (1-4) for incompressible, electrically conducting, viscous fluid in the presence of an applied, uniform magnetic field of strength B. The set of equations includes the continuity equation (1), momentum equation with the electromagnetic Lorentz force term on the right-hand-side (2), Ohm's law to compute the induced electric currents (3), and the electric potential equation for a multi-material domain (4):

$$\nabla \cdot \mathbf{u} = 0, \tag{1}$$

$$\rho \frac{\partial \mathbf{u}}{\partial t} + \rho \mathbf{u} \cdot \nabla \mathbf{u} = -\nabla \mathrm{p} + \nabla \cdot \mu \nabla \mathbf{u} + \mathbf{J} \times \mathbf{B}, \tag{2}$$

$$\mathbf{J} = \sigma(-\nabla \phi + \mathbf{u} \times \mathbf{B}), \tag{3}$$

$$\nabla \cdot (\sigma \nabla \phi) = \nabla \cdot (\sigma \mathbf{u} \times \mathbf{B}). \tag{4}$$

Here, **u**, **J**, and **B** are the velocity, electric current density, and applied magnetic field vectors respectively and p and ϕ are the pressure and electric potential scalars. Equation (4) is derived by taking the divergence of Eq. (3) with the added stipulation that electrical current density is divergence free ($\nabla \cdot \mathbf{J} = 0$). It is assumed that the magnetic Reynolds number (ratio between convection and diffusion of the magnetic field) is small, such that the induced magnetic field is negligible compared to the applied one.

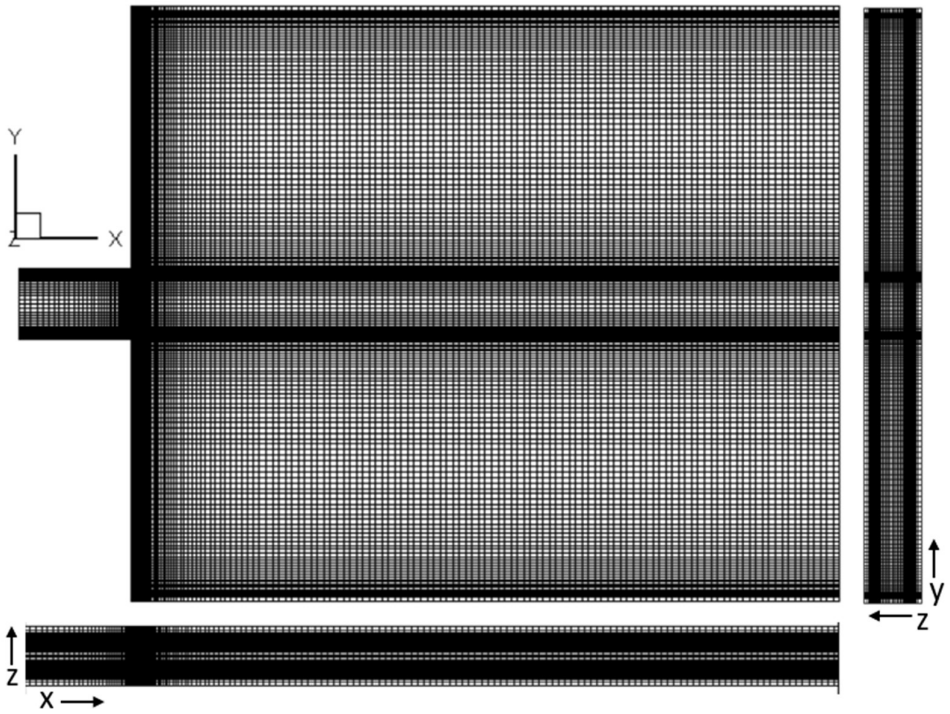

Figure 2. The computational mesh has 2.56 million cells. The number of cells in the x, y and z directions is 180, 268, and 53.

2.2. *Computational mesh*

Equations (1, 2) and (4) are solved numerically on a non-uniform rectangular mesh (Fig. 2). Similar meshes have previously been evaluated in a mesh refinement study using the same solver and similar parameters in [14]. We ensured that there are at least 5 nodes inside all Hartmann layers on the walls perpendicular to the magnetic field and 12 nodes inside each side layer on the walls parallel to the magnetic field. Also, the mesh has been refined along the axial direction in the vicinity of the sudden contraction/expansion where internal shear layers are expected to exist [6,8,14,16,17]. As a result, the computational mesh has 2.56 million cells.

2.3. *Initial and boundary conditions*

The flow field is initially uniform with speed U. A uniform flow condition is used as the inlet boundary condition. The outlet boundary condition is in the form $\frac{\partial}{\partial x} = 0$ for all variables except pressure. The pressure is set to zero at the outlet and a Neumann condition is used at the inlet. The no-slip condition is enforced at all fluid-wall interfaces. Components of electrical current density normal to the simulation domain boundary are set to zero along the boundary as all the duct walls are non-conducting. To ensure faster convergence, the flow and electric potential fields obtained at lower Re and Ha are used as initial conditions in computations for higher parameters.

2.4. *Numerical solver*

Simulations were performed using the HIMAG solver (HyPerComp Incompressible Magnetohydrodynamic Solver for Arbitrary Geometries). Details regarding the formulation and validation of the HIMAG code can be found elsewhere (e.g. [18, 19]). HIMAG is a three-dimensional, unstructured grid-based MHD flow solver developed over the last decade by a US software company named HyPerComp, with support from UCLA. The numerical approach is based on finite-volume discretization using a collocated arrangement (all unknowns are located at the cell centers) with second-order accuracy in space and time. The mass conservation is satisfied, and the pressure field is evaluated using a four-step projection method with the semi-implicit Crank–Nicolson formulation for the convective and diffusion terms. A charge conserving consistent scheme developed in Ref. [20] is applied to accurately compute the electric potential and the electric current density at high Hartmann numbers. The solver algorithms are parallelized using the Message Passing Interface (MPI) architecture, thereby making the solver capable of being run on large computational clusters.

3. Summary of the previous results for the inlet manifold

Steady state solutions were computed in [14] for a range of flow and geometry parameters in order to better understand the physical mechanisms that characterize the 3D pressure drop ΔP_{3D} and flow distribution in the prototypic inlet manifold of a PbLi blanket in order to deduce correlations for ΔP_{3D}. The inlet manifold flow was simulated where liquid metal enters the manifold of height $2a$ through the feeding duct of width $2d$ before entering the expansion region, which has length L_{exp} and toroidal width $2b$. From the expansion region, the flow proceeds into three or more parallel channels of the width $2h$ each. The flow occurs in a uniform transverse (toroidal) magnetic field B.

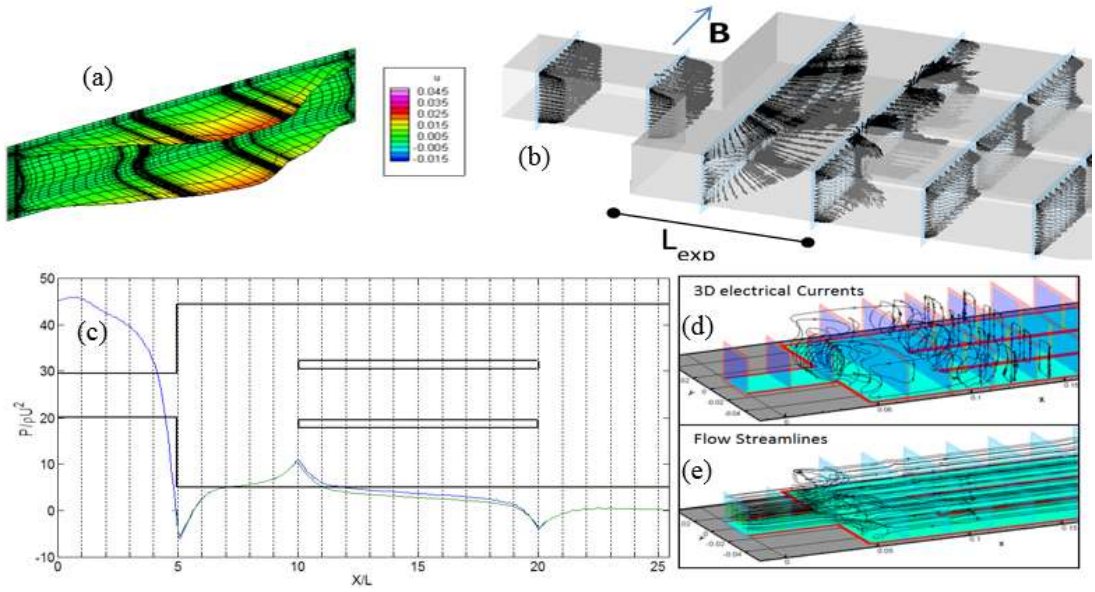

Figure 3. Results for steady MHD flow through a 3D inlet manifold featuring expansion with non-conducting walls and strong transverse magnetic field at *Ha*=2190 and *Re*=625 [14]. (a) Velocity profile in the expansion region. (b) Velocity vectors. (c) Pressure distribution along the centerlines of the channels. (d) Electrical current tracers. (e) Flow tracers.

As discussed in [14], the flow distribution in this geometry is controlled by the flow becoming dominantly two-dimensional in a strong magnetic field (the flow becomes more uniformly distributed in the direction of the applied magnetic field as magnetic field is increased) and by the formation of side-layer jets (Fig. 3a), which decay exponentially in the flow direction. As L_{exp} decreases, a larger portion of the flow will enter the central channel since the jets carry more flow in the center than the sides. The flow distribution becomes more uniform as the Hartmann number or L_{exp} increases. It was also concluded that almost all MHD pressure drop occurs in the expansion region of the manifold, while the MHD pressure drops associated with the flow redistribution from the expansion region into parallel poloidal ducts and that due to the radial-poloidal change in the flow direction are significantly smaller. This conclusion allowed for further reduction of the MHD pressure drop analysis to focusing on the flow in the expansion region only as shown in Fig. 1. Totally 96 cases were computed in [14] for $1000 < Ha < 6570$, $50 < Re < 2500$ and $4 < r_{exp} < 12$.

Two flow regimes, VE for $Re/\sqrt{Ha} < 3$ and IE for $Re/\sqrt{Ha} > 3$, were confirmed as supported by the aforementioned analysis of 2D expansions, and formulas for 3D MHD pressure drop had been determined for electrically insulated inlet manifolds as follows:

$$VE\ regime: \Delta P_{3D} = \frac{\rho U^2}{2}\left(k_{ve} N Ha^{-1/2} + d_{ve}\right) \text{ for } \frac{Re}{\sqrt{Ha}} < 3, \quad (5)$$

$$IE\ regime: \Delta P_{3D} = \frac{\rho U^2}{2}\left(k_{ie} N^{2/3} + d_{ie}\right) \text{ for } \frac{Re}{\sqrt{Ha}} > 3. \quad (6)$$

Here, k_{ve}, d_{ve}, k_{ie}, and d_{ie} are functions of the expansion ratio, r_{exp}:

$$k_{ve} = 0.31 r_{exp} + 3.08, \quad (7)$$

$$d_{ve} = 342.92 r_{exp} - 1563.85, \quad (8)$$

$$k_{ie} = 0.33 r_{exp} + 1.19, \quad (9)$$

$$d_{ie} = -11.55 r_{exp}^{\ 2} + 85.43 r_{exp} - 264.39. \quad (10)$$

Equations (5) and (6) together with Eqs. (7-10) serve as a pressure model that describes the behavior of the 3D MHD pressure drop in both the viscous-electromagnetic and inertial-electromagnetic regimes in the inlet manifold.

4. Results for the contraction flows and discussion

4.1. *Flow development in the duct with contraction*

Similar to the analysis in [14] for the inlet manifold, the present study for the outlet manifold doesn't include the parallel channels and focuses on the contraction region only, where the most pressure drop of the entire manifold pressure drop occurs. The flow behavior in MHD duct flows featuring a sudden contraction along the magnetic field direction is illustrated here using the present computations for a selected case of *Ha*=2500, *Re*=500 and contraction ratio 10 as shown in Fig. 4 . Flow enters the wide end of the duct uniformly (Fig. 4a) and quickly becomes fully developed and quasi-two-dimensional (Fig. 4b), demonstrating distinctive Hartmann layers, side layers and a near-uniform core. Nearer the expansion region, abrupt 3D flow redistribution occurs as seen in Fig. 4c.

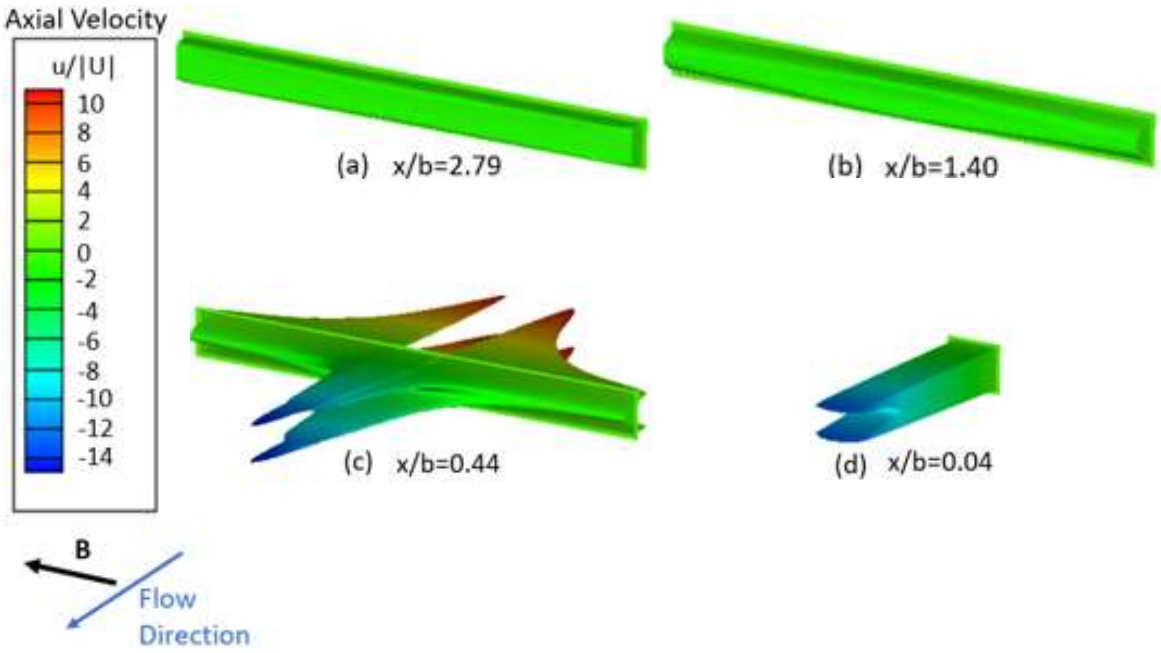

Figure 4. Axial velocity profiles of a sudden contraction flow at *Ha*=2500, *Re*=500 and the contraction ratio 10. The locations of the profiles are also shown in Fig. 1.

Namely, the incoming flow migrates away from the sidewalls and the side layers forming a reversed flow in a wide duct slightly upstream of the sudden expansion. At the same time, when the liquid

enters the narrow duct, two high velocity jets are formed in the narrow duct at the walls parallel to the magnetic field right downstream of the sudden contraction. These abrupt changes in the flow occur quickly over a very short distance, much lesser than the characteristic duct size, indicating to the formation of the internal Ludford-type boundary layer [17]. Inside the narrow duct, the jets attached to the sidewalls (Fig. 4d) fade as the flow quickly develops into a Shercliff flow [21].

This flow behavior near the sudden contraction reminds the flow in the expansion region of the same dimensions as computed in [14] and summarized here in Section 3, where the abrupt flow changes and formation of the Ludford layer were also observed for the same flow parameters. However, as demonstrated in computations in [13], the flow patterns between the expansion and contraction flows and associated pressure drops are not exactly the same as the inertial forces are, in general, not reversible. In fact, as seen from the present studies, the differences become more visible as the flow changes from the VE to the IE regime. These differences are further analyzed in the next sections.

4.2. *MHD pressure drop in the contraction flows compared to the expansions*

The computations of the MHD flow through a contraction were performed for $50 < Re < 1500$, $2500 < Ha < 5475$, and contraction ratio 10. Totally 14 cases have been computed. A comparison of the dimensionless pressure scaled by the dynamic head between the expansion and contraction is shown in Fig. 5 for the IE regime at Ha=2500 and Re=500, for which the highest difference of ~8% in the entire pressure drop in the duct with sudden contraction was observed.

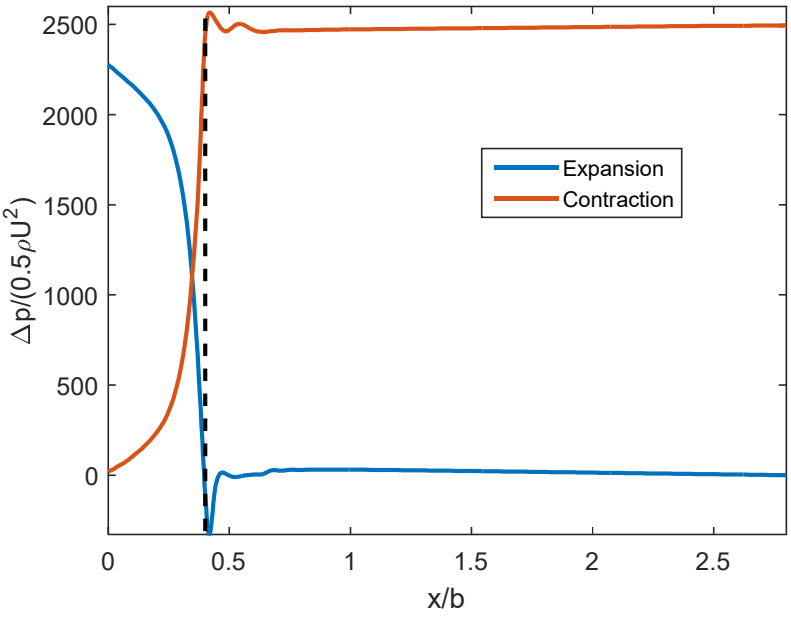

Figure 5. Axial pressure distributions at Ha=2500, Re=500 for a sudden expansion flow (flow enters from the left) and a sudden contraction flow (flow enters from the right). The dashed vertical line shows the location of the sudden change in duct aspect ratio.

Both curves in Fig. 5 exhibit near-constant pressure gradients when approaching their outlets (x/b=0 and x/b=2.8 for expansion and contraction cases respectively). More detailed analyses shows that these pressure gradients are close to those in a fully-developed Shercliff flow in a non-conducting

duct [21], indicating that the flow development occurs over a short distance of a few characteristic lengths. However, each pressure curve features a large 3D MHD pressure drop near the sudden change in duct width, which accounts for the majority of the total pressure drop across each duct. It is notiacable that the contraction flow demonstrates a slightly higher pressure peak near the sudden change of the flow geometry compared to the expansion flow. Except for the pressure peak and a short adjacent region, the two pressure curves look completerly symmetrical.

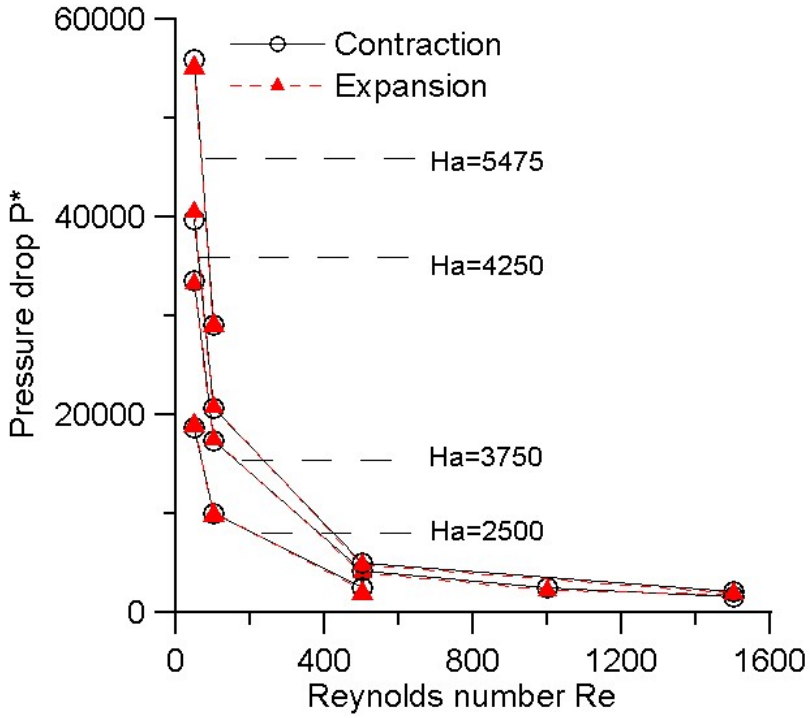

Figure 6. Effect of the Reynolds number on the 3D MHD pressure drop in a duct with sudden changes in the cross-sectional area for several Hartmann numbers.

To further investigate how the 3D MHD pressure drop across sudden contractions can differ from the sudden expansions at various *Ha* and *Re* numbers, the computed data for the 14 pairs are plotted in Figs 6 and 7. Figure 6 shows the dimensionless pressure drop $P^* = \frac{\Delta p}{0.5\rho U^2}$ (where Δp is the pressure difference between the inlet and outlet boundaries of the duct) as a function of the Reynolds number for several Hartmann numbers. Clearly, the difference between the contraction and expansion data is very small. In Fig. 7, the same data for *P** are plotted as a function of the Hartmann number. Visually, small differences can be seen at the highest *Re* of 1500 (at the bottom of the figure). The observed trends in the 3D MHD pressure drop in Figs. 6 and 7 are similar to the observations in Refs. [12] and [13] by Kimamaru at lower Hartmann numbers.

Of all the cases computed, the quantitative percentage difference between pressure drops of expansion and contraction cases are less than 2% in the VE regime and greater than 4% in the IE regime, with a maximum of about 8% at *Ha*=3750, *Re*=1500. In the IE regime, all contraction cases featured larger pressure drops than their respective expansion cases. The observation that differences between expansion and contraction flows are larger in the IE regime than in the VE regime can be explained by the contribution of the inertial force term in Eq. (2). In contrast to the inertial forces, viscous and electromagnetic Lorentz force are reversable and so changing the flow direction has only small effect on the pressure drop in the VE regime.

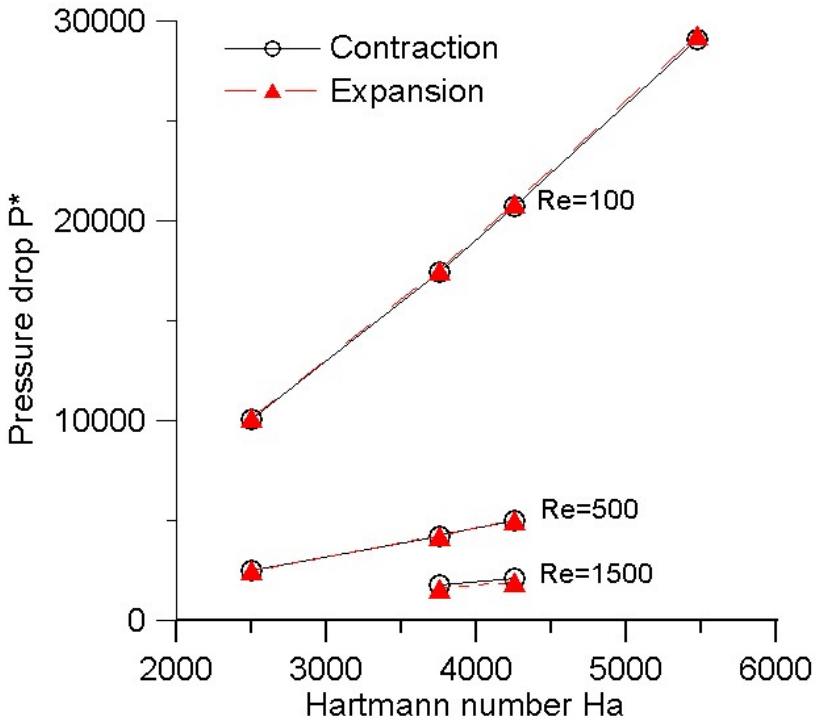

Figure 7. Effect of the Hartmann number on the 3D MHD pressure drop in a duct with sudden changes in the cross-sectional area for several Reynolds numbers.

It should be noted that the present analysis of the MHD pressure drop is limited to *Ha* and *Re* numbers significantly lower than those in the blanket applications. As a matter of fact, the parameter range employed in the present study is closer to experimental studies. Such limitations are related to the need of very expansive computations at higher *Ha* and *Re* that were not affordable in the present research project. A question arises about the degree to which the present conclusions are valid for higher magnitudes of the flow parameters. There are two arguments that support the idea that the present conclusions and correlations can be used even for the blanket flows where $Ha \sim 10^4$ and $Re \sim 10^4$-10^5.

First, as shown in this study and also in the previous studies cited in this paper, the flow in a duct with a sudden change in the cross-sectional area, i.e. expansion or contraction, is fully controlled by the formation of the Ludford-type internal boundary layer. This phenomenon is fully described by the dimensionless parameters *Ha* and *Re*. In particular, the parameter $Re/\sqrt{Ha}$ is of special importance as it can be used to distinguish between the VE and IE regimes. In both the blankets applications and to major degree in the present studies, this parameter is higher than 3, suggesting the same IE flow regime, such that the correlations obtained at relatively low *Ha* and *Re* for this regime seem to remain applicable to the flows at higher numbers.

Second, we have compared the present results and conclusions with the results in Ref. [22] where the entire DCLL blanket module was simulated, including MHD flows in the inlet and outlet manifolds at Hartmann and Reynolds numbers significantly higher than *Ha* and *Re* of the present study. Namely, in Ref. [22], $Re=3.2\text{x}10^5$ and $Ha=3.3\text{x}10^4$, while the expansion/contraction ratio was 6. In such conditions, the parameter $Re/\sqrt{Ha}$ in Ref. [22] was very high ~1760, suggesting strong inertial effects. Similar to the present results, the computations in Ref. [22] demonstrated pronounced

3D flow features in the nearest vicinity of the sudden change of the duct geometry. Nevertheless, unlike the present study, the manifold flows in Ref. [22] were found to be unsteady. 3D velocity spikes were observed near the expansion and contraction that resembled pulsations in turbulent flows. However, the 3D features were quickly damped at a short distance downstream from the expansion or contraction such that over the major manifold length, the flow appeared in the Q2D form. Interestingly, the comparison of the MHD pressure drop in [22] between the inlet and outlet manifolds revealed a 6% difference, which is very similar to the maximum difference of 8% in the present study. Applying formulas (6), (9) and (10) to the outlet manifold flow simulated in Ref. [22] results in the pressure drop of 0.105 MPa, while computatipons in [22] suggest 0.116 MPa. Taking into account the complexity of the MHD flow, high magnitudes of the flow parameters and also some small differences in the manifold design in [22] compared to the manifold model in the present study, one can conclude that the proposed Eqs. (5-10) provide acceptable accurcy (from the engineering viepoint) not only under experimental but also under the full blanket conditions.

4.3. *Comparison of the MHD flow patterns between contraction and expansion flows*

As noticed in [13], in the flows through a sudden contraction oriented in the direction of applied magnetic field, the loss coefficient takes a positive and large value in all the cases performed in that study. The loss coefficient generally becomes slightly larger than that in the case of corresponding channel expansion and is increased with the Hartmann number and decreased with the Reynolds number. This suggests that the MHD pressure drop in the contraction flows is slightly higher compared to the expansions. This trend was also well confirmed in the present studies showing higher pressure losses in the flow in the duct with contraction, providing $Re/\sqrt{Ha} > 3$, such that the flow regime is inertial-electromagnetic. Besides such small differences in the MHD pressure drop, it is interesting to look for any noticeable differences in the flow patterns.

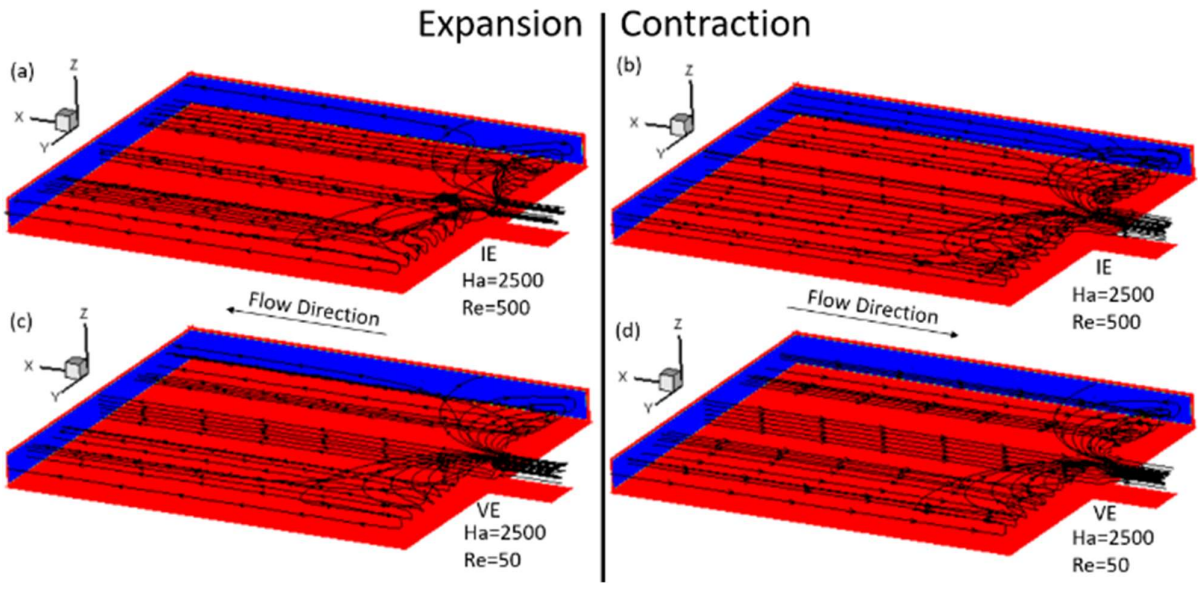

Figure 8. Velocity streamlines at *Ha*=2500 reveal the 3D MHD flow structure near each sudden change of the duct cross-sectional area for both (a,c) expansions and (b,d) contractions. (a,b) *Re*=500, (c,d) *Re*=50.

Streamlines of MHD flows in ducts featuring a sudden expansion and a sudden contraction are compared in Fig. 8 for *Ha*=2500 and two Reynolds numbers, *Re*=50 and 500, to represent flows in the VE regime and IE regime respectively. In all 4 cases, a 3D MHD flow structure exists near the sudden change of the duct that redistributes flow along the magnetic field direction via thin layers attached to the sidewalls.

In the IE regime (Fig. 8a,b), there are visually observed differences between the streamlines of the expansion and contraction cases. The largest difference is the existance of stationary vortex tubes in the bulk of the expansion flow, just downstream of the expansion, which do not appear in the contraction flow. In the VE regime (Fig. 8c,d), the streamlines look qualitatively the same for both expansion and contraction cases. The flow distribution details are further illuistrated in Fig. 9 where streamlines are shown on the *y*=0 centerplane for the same 4 cases. Again, differences between expansion and contraction flows are seen to be larger in the IE regime than in the VE regime. Figure 9a clearly shows two stationary vortex tubes in the expansion case while no vortices are seen in the counter case in Fig. 9b for the contracting flow.

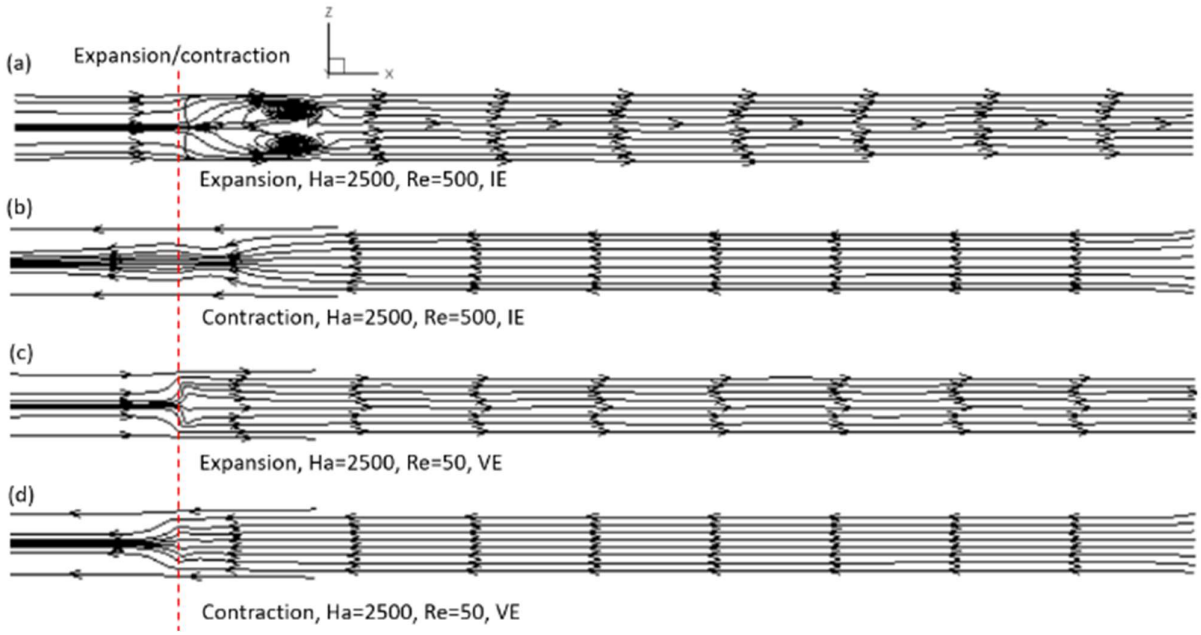

Figure 9. Velocity streamlines on the *y*=0 center plane at *Ha*=2500 for both (a,c) expansions and (b,d) contractions. The vertical dashed line marks the location of the sudden change in duct aspect ratio. (a,b) *Re*=500, (c,d) *Re*=50.

5. Conclusions

HIMAG code was used to simulate MHD flows in electrically insulated ducts featuring sudden contractions and expansions to explore the effect of each geometry on 3D MHD pressure drop of manifolds of a LM fusion blanket. In the present 3D computational studies for contractions that occur in the plane parallel to the applied magnetic field, $50 < Re < 1500$, $2500 < Ha < 5475$, and the expansion/contraction ratio is 10. We found that reversing the flow direction (thus changing a contraction into an expansion and *vice versa*) caused differences in pressure drop less than 2% if the flow regime is viscose-electromagnetic (at $Re/\sqrt{Ha} < 3$) and 4-8% in the case of the inertial-electromagnetic flow regime (at $Re/\sqrt{Ha} > 3$). The differences are associated with the inertial forces, which are unlike viscose and electromagnetic forces, are irreversible. Slightly higher 3D pressure

drops were observed in the contraction flows. These observations are consistent with the previous studies at lower flow parameters in [12, 13] and significantly higher blanket-relevant flow parameters in [22]. All these observations and comparisons suggest that Eqs. (5-10) for the 3D MHD pressure drop obtained earlier by the authors for the inlet manifold can also be recommended for the design and analysis of outlet manifolds. A relatively small safety factor of ~1.1 could be recommended in the engineering blanket studies to account for slightly higher pressure drops in contractions compared to expansions.

Acknowledgements

This work was performed with support from a subcontract between UCLA and ORNL #4000171188 and from the US DOE grant DE-SC0020979 . The numerical efforts of this research used resources of the National Energy Research Scientific Computing Center (NERSC), a U.S. Department of Energy Office of Science User Facility operated under Contract No. DE-AC02 05CH11231. Special thanks to Dr. Peter Huang from HyPerComp Inc for the technical support he provided in getting HIMAG to run on NERSC computers.

References

[1] S. Smolentsev, R. Moreau, L. Bühler, C. Mistrangelo, MHD thermofluid issues of liquid-metal blankets: phenomena and advances, Fusion Eng. Des., 85 (2010) 1196-1205.

[2] S. Smolentsev, N.B. Morley, M. Abdou, S. Malang, Dual-coolant lead-lithium (DCLL) blanket status and R&D needs, Fusion Eng. Des., 100 (2015) 44-54.

[3] M. Abdou, A. Ying, N. Morley, K. Gulec, S. Smolentsev, M Kotschenreuther, S Malang et al., On the exploration of innovative concepts for fusion chamber technology, Fusion Eng. Des., 54 (2001) 181-247.

[4] S. Smolentsev, C. Wong, S. Malang, M. Dagher, M. Abdou, MHD considerations for the DCLL inboard blanket and access ducts, Fusion Eng. Des., 85 (2010) 1007-1011.

[5] S. Smolentsev, T. Rhodes, G. Pulugundla, C. Courtessole, M. Abdou, S. Malang, M. Tillack, C. Kessel, MHD thermohydraulics analysis and supporting R&D for DCLL blanket in the FNSF, Fusion Eng. Des., 135 (2018) 314-323.

[6] S. Molokov, Liquid Metal Flows in Manifolds and Expansions of Insulating Rectangular Ducts in the Plane Perpendicular to a Strong Magnetic Field, KfK-5272, Kernforschungszentrum Karlsruhe, 1994.

[7] L. Bühler, Inertialess Magnetohydrodynamic Flows in Expansions and Contractions, FZKA 6904, Kernforschungszentrum Karlsruhe, 2003.

[8] C. Mistrangelo, Three-dimensional MHD Flow in Sudden Expansions, Ph.D. Thesis, FZK, 2006.

[9] C. N. Kim, Liquid metal magnetohydrodynamic flows in an electrically conducting rectangular duct with sudden expansion, Comput. Fluids, 89 (2014) 232–241.

[10] C. N. Kim, A liquid metal magnetohydrodynamic duct flow with sudden contraction in a direction perpendicular to a magnetic field, Comput. Fluids, 108 (2015) 156–167.

[11] J. Feng , Q. He, H. Chen, et al., Numerical investigation of magnetohydrodynamic flow through sudden expansion pipes in liquid metal blankets, Fusion Eng. Des., 109-111 (2016) 1360–1364.

[12] H. Kumamaru, Numerical analyses on liquid-metal magnetohydrodynamic flow in sudden channel expansion, J. Nucl. Sci. Technol., 54 (2017) 242–252.

[13] H. Kumamaru, Numerical analyses on liquid-metal magnetohydrodynamic flow in sudden channel contraction, J. Nucl. Sci. Technol., 54 (2017) 1300–1309.

[14] T. Rhodes, S. Smolentsev, M. Abdou, Magnetohydrodynamic pressure drop and flow balancing of liquid metal flow in a prototypic fusion blanket manifold, Physics of Fluids, 30 (2018) 057101.

[15] S. Smolentsev, S. Badia, R. Bhattacharyay, L. Bühler, L. Chen et al., An approach to verification and validation of MHD codes for fusion applications, Fusion Eng. Des., 100 (2015) 65-72.

[16] L. Bühler, S. Horanyi, Experimental Investigations of MHD Flows in a Sudden Expansion, KfK-7245, Kernforschungszentrum Karlsruhe, 2006.

[17] J. Hunt, S. Leibovich, Magnetohydrodynamic flow in channels of variable cross-section with strong transverse magnetic fields, J. Fluid Mech., 28 (1967) 241-260.

[18] S. Smolentsev, N. Morley, M. Abdou, R. Munipalli, R. Moreau, Current approaches to modeling MHD flows in the dual coolant lead lithium blanket, Magnetohydrodynamics, 42 (2006) 225-236.

[19] R. Munipalli, S. Shankar, M.-J. Ni, N. Morley, Development of a 3-D Incompressible Free Surface MHD Computational Environment for Arbitrary Geometries: HIMAG, DOE SBIR Phase-II Final Report, 2003.

[20] M.-J. Ni, R. Munipalli, N. Morley, P. Huang, M. Abdou, A current density conservative scheme for incompressible MHD flows at a low magnetic Reynolds number. Part I: On a rectangular collocated grid system, J. Comput. Phys., 227 (2007) 174–204.

[21] J. Shercliff, Steady motion of conducting fluids in pipes under transverse magnetic fields, Mathematical Proceedings of the Cambridge Philosophical Society, 49 (1953) 136-144.

[22] L. Chen, S. Smolentsev, M.-J. Ni, Toward full simulations for a liquid metal blanket: MHD flow computations for a PbLi blanket prototype at $Ha \sim 10^4$, Nucl. Fusion, 60 (2020) 076003.